Marine Micropaleontology 157 (2020) 101872

Contents lists available at ScienceDirect

Marine Micropaleontology

journal homepage: www.elsevier.com/locate/marmicro

Research paper

Evidence for rapid trace element alteration of planktic foraminiferal shells from the Panama Basin: Manganese adsorption during vertical transport

Catherine V. Davis*,[1], Claudia R. Benitez-Nelson

School of the Earth, Ocean, and Environment, University of South Carolina, Columbia, SC 29208, United States of America

A B S T R A C T

The trace elemental composition of planktic foraminifera shells serves as a proxy for understanding the physical environment in which foraminifera lived, but may also reflect chemical alterations that occur after death. Understanding how foraminiferal geochemistry varies across time, species, and after death is therefore essential for deconvolving ecological from diagenetic information and decoding the environmental signals contained within foraminiferal shells. We analyzed the trace elemental composition (Mg/Ca, Sr/Ca, Ba/Ca, Mn/Ca, and U/Ca) of four species of planktic foraminifera (*Globigerina ruber*, *Neogloboquadrina dutertrei*, *Globorotalia menardii*, and *Globorotaloides hexagonus*) from moored sediment traps (890, 2590, and 3560 m deep) in the Panama Basin collected over one calendar year (1979–1980). Shells recovered from the shallowest trap demonstrate moderate variability in trace elemental composition, both throughout the time series and between species. Most elemental ratios are not significantly influenced by depth, with the exception of Mn/Ca. Ratios of Mn/Ca are substantially higher in the 3560 m trap versus the 890 m trap, with increases with depth greater in the thin walled species *G. ruber* and *G. hexagonus*. Elevated Mn/Ca ratios are frequently noted in fossil foraminifera shells as the result of diagenesis within the sediment. Our results demonstrate the potential for Mn-enrichment of foraminiferal calcite, via Mn adsorption onto the surface of foraminiferal shells, within the water column during sinking and prior to deposition in the sediment.

1. Introduction

The trace element geochemistry of foraminfieral shells, particular the element to calcium ratios of elements such as Mg, Ba, Sr, B, and U, serves as an important tool for reconstructing past marine environments (see Lea, 1999; Katz et al., 2010 for reviews). However, straightforward interpretations of foraminiferal trace element geochemistry are complicated by preservation (e.g., Dekens et al., 2002; Pena et al., 2005; Pena et al., 2008; Sexton et al., 2006), species-specific differences in incorporation of, or exposure to, different trace elements (e.g., Allen et al., 2016; Anand et al., 2003; Cleroux et al., 2008; Regenberg et al., 2009), and biases associated with seasonality and changing depth habitat (e.g., Fraile et al., 2009; Jonkers and Kucera, 2015). One of the most confounding issues in interpreting trace elemental paleoproxies is the potential for diagenetic alteration of the original shell geochemistry by calcite overgrowths, recrystallization, and the selective dissolution of original calcite after sediment burial (e.g., Boyle, 1983; Dekens et al., 2002; Barker et al., 2003; Pena et al., 2005; Sexton et al., 2006; Pena et al., 2008).

Removal of post-mortem diagenetic phases from shell surfaces is a routine aspect of trace element analyses, taking the form of chemical or mechanical 'cleaning' (Boyle and Keigwin, 1985; Barker et al., 2003), flow-through systems (Benway et al., 2003), or analytical removal by laser ablation (Reichart et al., 2003; Marr et al., 2013). The goal of these approaches is to minimize the influence of diagenetic, sedimentary, and organic materials on the measurement of paleoceanographically significant elements such as Mg, Ba, or B. Success of these approaches is often evaluated by using the elements Mn, Al, and Fe, as guides to assess the effectiveness of oxide and clay removal (Boyle, 1983; Barker et al., 2003; Pena et al., 2005, 2008). Elements associated with post-depositional alteration are also occasionally used as proxies for the depositional environment. For example uncleaned shells are sometimes analyzed for the trace element content of post-depositional overgrowths (e.g., U/Ca and Mn/Ca) as proxies for bottom water redox conditions (e.g., Palmern and Elderfield, 1986; Boiteau et al., 2012; Gottschalk et al., 2016; Umling and Thunell, 2018), assuming that the original calcite of surface-dwelling foraminifera contains comparably negligible quantities of these elements.

One less frequently considered source of post mortem alteration are overgrowths, adsorption, and dissolution that may occur while shells sink through the water column. Takahashi (1984) estimate that a foraminifera settling to 3800 m from surface waters spends 3–12 days in the water column, with smaller, lighter foraminifera sinking more slowly. During this period, a shell could be exposed to a wide range of water chemistries, including changes in carbonate saturation state, redox state, and water masses with otherwise differing chemistries.

* Corresponding author.
E-mail address: catherine.davis@yale.edu (C.V. Davis).
[1] Present Address: Department of Geology & Geophysics, Yale University, New Haven, CT 65011.

https://doi.org/10.1016/j.marmicro.2020.101872
Received 22 October 2019; Received in revised form 3 March 2020; Accepted 31 March 2020
Available online 02 April 2020

Alternatively, some shells may be transported via fecal pellets, or within aggregate particles or marine snow. As a result, shells may interact with microbial communities, organics either within or outside of the shell, or water chemistries unlike those experienced during calcification. Any of these eventualities could impact the trace element composition of a shell prior to deposition in the sediment.

Relatively little attention has been paid to the early stage of diagenesis that may occur as shells sink through the water column. However, recent laboratory experiments have shown the potential for rapid alteration (dissolution and recrystallization) of the trace element composition of foraminiferal shells on relatively short timescales of weeks to months, with younger shells more susceptible than fossils (Chanda et al., 2019). Gibson et al. (2016) also found evidence for rapid alteration of foraminiferal calcite in sediment traps from the Gulf of Tuhantapec. Alteration in this later case was associated with visible overgrowths on the inner and outer shell surface, which were interpreted as having developed within the sediment trap cups.

The aim of this study is to describe the trace element composition of planktic foraminifera collected during a yearlong sediment trap deployment in the Panama Basin. The Panama Basin is of particular interest as foraminifera from sediments in the region have variable preservation and diagenetically altered trace element ratios, particularly with regards to high Mn/Ca (e.g., Boyle, 1983; Pena et al., 2005, 2008; Tachikawa et al., 2013; Umling et al., 2018). Four species of foraminifera are examined from three deep moored sediment traps that cross a strong oxygen gradient. This allows for a comparison of trace elemental variability between seasons and species, and for testing the potential for early diagenetic alteration of foraminiferal trace metal geochemistry occurring within the water column.

2. Methods

2.1. Panama Basin sediment trap

Samples from the Panama Basin were collected from a sediment trap deployed at 5° 21′ N, 81° 53′ W between December of 1979 and November of 1980 in a water depth of ~3860 m (Fig. 1). The Panama Basin is enclosed by Central and South America to the East and Southeast and the Cocos and Carnegie Ridges to the Northwest and South respectively. An intense Oxygen Minimum Zone cuts across intermediate water depths and the Panama Basin sediment traps were deployed at 890 m, 2590 m, and 3560 m across a range of dissolved oxygen (Fig. 2). Each trap was equipped with 6 cups, each with a ~ 2 month collection period, and injected with sodium azide to poison and preserve organic material. After trap recovery, individual foraminifera were isolated from sediment trap material and stored in micropaleontological slides. Due to trap failures, material is only available for cups 1–4 in the two deeper traps (December–August).

2.2. Foraminifera selection

Four species of planktic foraminifera were selected for analyses, *Globigerina ruber* (sensu stricto), *Neogloboquadrina dutertrei*, *Globorotalia menardii*, and *Globorotaloides hexagonus*. Foraminifera species were targeted based on their availability in trap material and to include a range of morphologies and depth habitats. Foraminifera were separated based on sieve fraction (250–355 μm, 355–500 μm, and > 500 μm) prior to analyses, with each sample containing between 1 and 25 shells (Supplemental Table 1). Samples were weighed, gently crushed in a microcentrifuge tube, and cleaned to remove any residual organic matter by submergence in a 1:1 mixture of H_2O_2 and NaOH in a warm water bath (~65 °C) for 10 min (Mashiotta et al., 1999). During this period, samples were sonicated 4 times for 10s. Samples were then triple rinsed in deionized water to remove reagents. Samples of *G. hexagonus* did not contain enough calcite to be reliably analyzed in solution, nor did those that contained only single foraminiferal shells. These individuals (n = 33) were cleaned as described above, but without crushing (Supplemental Table 1).

2.3. ICP-MS and SEM

Trace element analyses were carried out using a Thermo Finnegan Element 2 in the Center for Elemental Mass Spectrometry (CEMS) at the University of South Carolina. Samples prepared for solution analyses were dissolved in 1% nitric acid and then diluted in a matrix of 2% nitric acid to a consistent concentration of 20 ppm Ca. Dissolved samples were run along with standard solutions, containing 20 ppm Ca and varying concentrations of other analytes. Analytes for solution analyses included ^{25}Mg, ^{43}Ca, ^{55}Mn, ^{87}Sr, ^{137}Ba, and ^{238}U. A consistency standard was analyzed 10 times across multiple analytical sessions and gave standard deviations of ± 0.02 mmol/mol for Mg/Ca, ± 4.3 μmol/mol for Mn/Ca, ± 0.01 mmol/mol for Sr/Ca, ± 0.08 μmol/mol for Ba/Ca and ± 1.17 ηmol/mol for U/Ca.

Samples introduced by laser ablation were run using a Photon Machines 193 nm ArF laser with an ANU HelEx dual-volume laser ablation cell system coupled to the same Thermo Finnegan Element 2 used for solution analyses. Foraminifera were ablated using a 65 μm spot size at 3 Hz and a fluence of 1.62 J cm^{-2}. Analytes for these foraminifera were ^{25}Mg, ^{43}Ca, ^{55}Mn, ^{87}Sr, and ^{137}Ba, with standard glasses NIST 610 and NIST 612 ablated every ~10 samples and used for drift correction. Data from laser ablation analyses were processed using the LATools software (Branson et al., 2019). Unless otherwise stated, all data is presented as a combination of solution values and the sample means of laser ablation data.

A subset of individual *G. ruber* and *N. dutertrei* shells from the 890 m and 3560 m sediment traps were also imaged by Scanning Electron Microscopy to identify visible signs of diagenetic alteration, such as textured overgrowths. These individuals were mounted on carbon tape, gold sputter coated, and imaged on a Tescan Vega3 Scanning Electron Microscope in the Electron Microscopy Center at the University of South Carolina.

3. Results

3.1. Trace element variability with time in Panama Basin

Our analysis of trace element variability over time focuses on the sediment trap record at 890 m due to the fewer number of samples from the lower trap cups. Where cup means are reported, they have been weighted for the number of individuals in each sample analyzed. No species of foraminifera showed a significant difference (p value < .05) in trace elemental composition with size fraction (Supplemental Fig. 1).

3.1.1. Mg/Ca

Mg/Ca values were largely consistent within species throughout the year. To test for trace element variability between different populations, a Kruskal-Wallis test was used, followed by a Dunn's test (Dunn, 1961). These non-parametric approaches are preferred as they account for the inherent potential for non-normality in our dataset. Application of a number of paleotemperature equations (Nurnberg et al., 1996; Elderfield and Ganssen, 2000; Anand et al., 2003; McConnell and Thunell, 2005; Regenberg et al., 2009) using the Mg/Ca values from *G. ruber* (4.0 to 7.9 mmol/mol) collected in the 890 m trap (Fig. 3a) results in temperatures ranging from 21 °C (Elderfield and Ganssen, 2000) to 37 °C (Anand et al., 2003). Most estimates fall in the 25–30 °C range with the exception of a single sample in February–March with an unusually high Mg/Ca of 13.6 mmol/mol. Application of the von Langen et al. (2005) relationship to *N. dutertrei* produces temperatures between 15 and 21 °C, with the exception of a single sample from December–January (Supplemental Table 1).

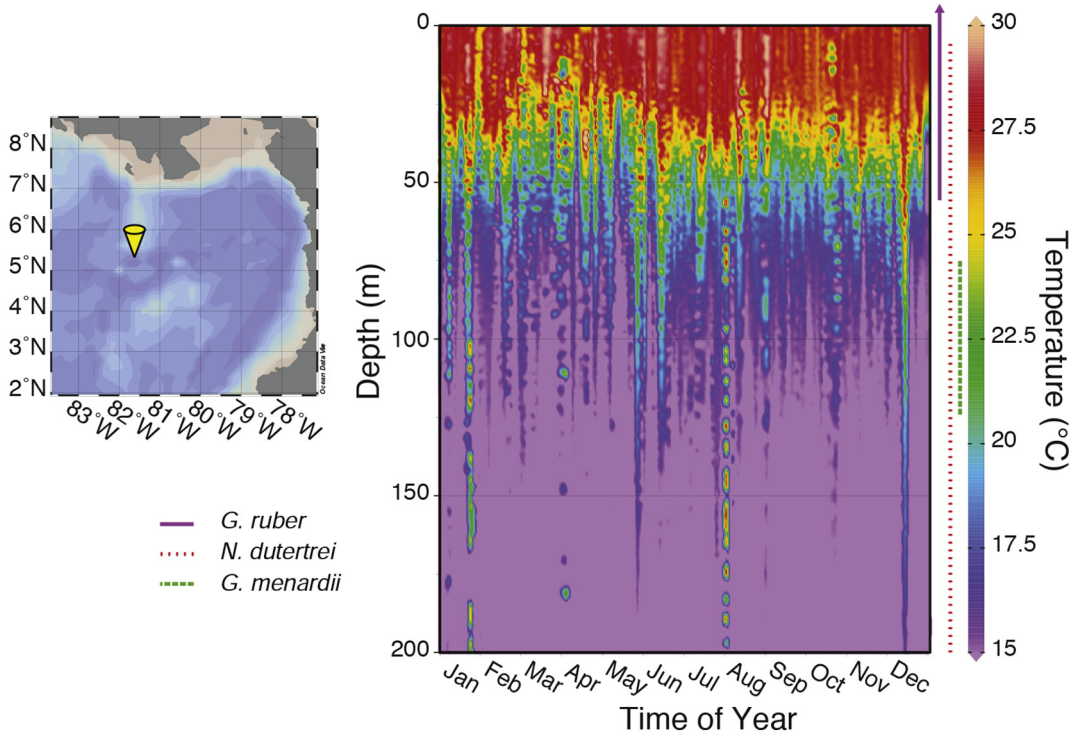

Fig. 1. The location of the sediment trap time series in the Panama Basin (left) along with temperature data for the upper 200 m compiled from available WOA18 data from the region plotted by depth and the day of the year (right). Data was plotted using Ocean Data Viewer. The temperature range at which calcification occurred as inferred from Mg/Ca is shown on the left for *G. ruber* (purple vertical line, Anand et al., 2003), *N. dutertrei* (red dotted vertical line, von Langen et al., 2005), and *G. menardii* (green vertical dashed line, Regenberg et al., 2009). (For interpretation of the references to colour in this figure legend, the reader is referred to the web version of this article.)

3.1.2. Sr/Ca

In *G. ruber,* Sr/Ca is lowest in October–November (mean = 1.35 mmol/mol) and reaches a peak in June–July (mean = 1.56 mmol/mol) (Fig. 3b). Sr/Ca in *N. dutertrei* is higher in April–May (mean = of 1.29 mmol/mol) than in summer and winter (means < 1.25 mmol/mol). *Globorotalia menardii* has fairly consistent Sr/Ca year-round (cup means between 1.24 and 1.26 mmol/mol) (Fig. 3b).

3.1.3. Ba/Ca

Ba/Ca is highest in December–May (cup means of 8.2 and 7.0 μmol/mol respectively) in *N. dutertrei*, before decreasing to consistently lower values for the rest of the year. Samples of *G. menardii* and *G. ruber* were only available from February–March, where Ba/Ca is highest in both species (means of 10.6 and 7.1 μmol/mol). Ba/Ca ratios decline below 5 μmol/mol from June to October (Fig. 3c).

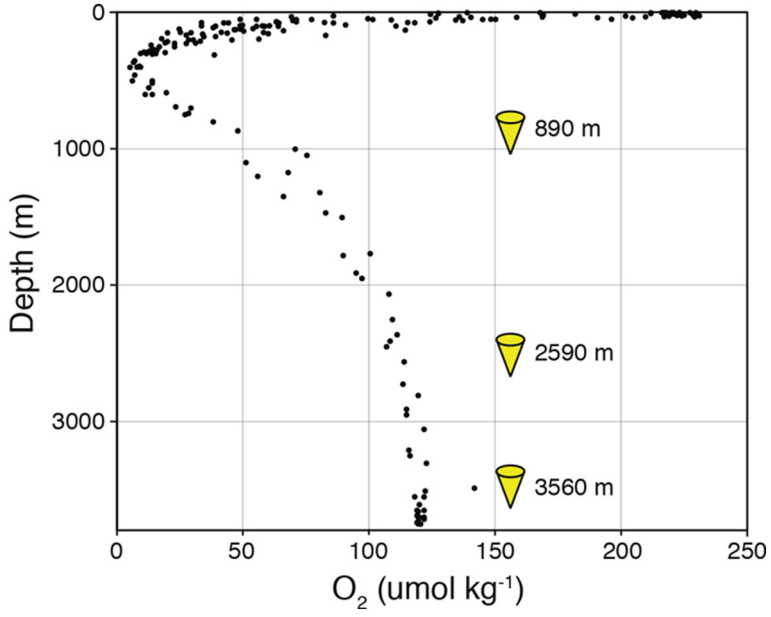

Fig. 2. Dissolved oxygen with depth compiled from WOA18 data available within 1 degree of the mooring site.

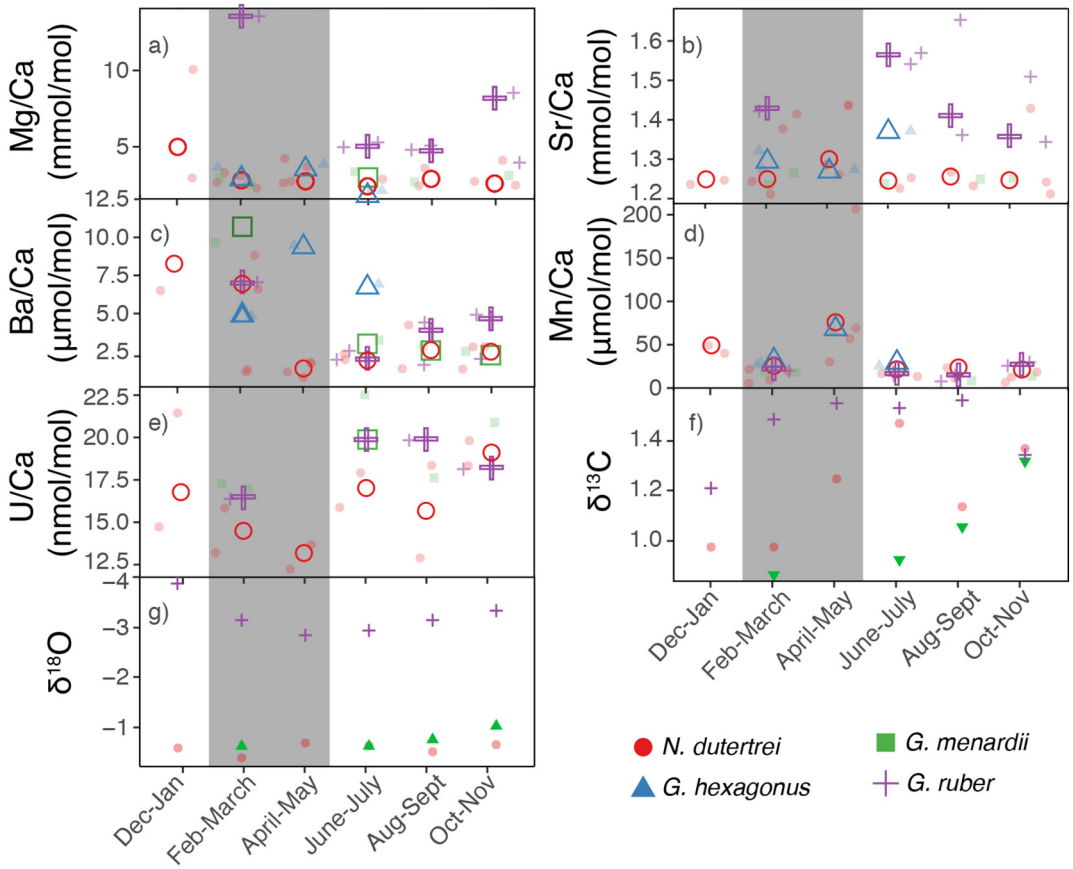

Fig. 3. Geochemistry of *N. dutertrei*, *G. hexagonus*, *G. menardii*, and *G. ruber* from the 890 m deep trap by cup. Data for $\delta^{18}O$ (f) and $\delta^{13}C$ (g) were previously published in Curry et al. (1983). No values for *G. hexagonus* are available for U/Ca (e), $\delta^{18}O$ (f), or $\delta^{13}C$ (g). Shaded regions denote the periods during which upwelling would be expected based on the climatological average. Weighted means for each cup are shown as large open symbols. Points have been jittered, distributed randomly in the x-dimension of each bin, for visibility.

3.1.4. Mn/Ca

Mn/Ca is low (< 26 μmol/mol) and consistent throughout the year in *G. ruber* and *G. menardii*. Mn/Ca ratios are highest in the only two species found in the June–July collection: *N. dutertrei* (cup mean of 69.2 μmol/mol, and maximum sample value of 206.6 μmol/mol) and *G. hexagonus* (cup mean of 64.1 μmol/mol) (Fig. 3d).

3.1.5. U/Ca

Values for U/Ca have not been reported for all samples due to high background levels of U during one solution ICP-MS run and exclusion from laser ablation analyses. However, a full year of U/Ca values was measured in *N. dutertrei*. The lowest values were measured in February–May (cup means of 14.4 and 13.1 nmol/mol in February–March and April–May respectively), with increasing values during the spring and summer (Fig. 3e). Data from both *G. ruber* and *G. menardii*, although sparse, confirm this general trend with the lowest values measured in samples from April–May (Fig. 3e).

3.2. Heterogeneity between species

Elemental composition varies between species. In particular, *G. ruber* has consistently higher Mg/Ca than the other species at all three depths (*p* values of 0.003, 0.005, and 0.005 respectively) (Fig. 4a). *Globigerinoides ruber* also has higher Sr/Ca ratios than *N. dutertrei* or *G. menardii* (Dunn's test p value = .008 and 0.004 respectively), but is not significantly different from *G. hexagonus* (p value = .25) at 890 m. These trends persist with depth in all three sediment traps (Fig. 4b). In the 890 m trap, Ba/Ca ratios are highest in *G. hexagonus*, followed by *G. menardii*, *N. dutertrei,* and *G. ruber* (Fig. 4c), although the differences between the four species are not significantly different. At 890 m Mn/Ca values are highest in *G. hexagonus*, followed by *N. dutertrei*, *G. ruber,* and *G. menardii*, although again populations are not found to be significantly different (*p* value = .16). This trend changes as Mn/Ca increases with depth, with populations of *N. dutertrei* having significantly less Mn/Ca than other species at both 2590 m (p value < .001) and 3560 m (p value = .007) (Fig. 4d). U/Ca ratios are consistently higher in *N. dutertrei* and *G. menardii* than in *G. ruber*, although the difference is only significant between *N. dutertrei* and *G. ruber* at 2590 m (*p* value = .01) (Fig. 4e).

3.3. Variability with depth

At the Panama Basin sediment trap mooring, no significant differences (*p* value < .05) are noted in the Mg/Ca, U/Ca or average shell weight of any species with depth (Fig. 4). Ba/Ca values increase systematically with depth, although populations are not found to be significantly different in any species (p value > .05) (Fig. 4c). It is important to note the potential influence of seasonality on these results, as collections from August to November are excluded from the deeper traps, such that higher Ba/Ca ratios from earlier in the year are overrepresented in deeper traps. Additionally, a small but significant increase is observed in the Sr/Ca values of *G. menardii* between 890 m (mean = 1.2 ± 0.01 mmol/mol) and 2590 m (mean = 1.3 ± 0.04 mmol/mol), regardless of whether August through November collections are excluded (p value = .03).

There is no significant correlation (*p* value < .05; Spearman correlation with Holm's correction for multiple hypothesis testing) between Mn/Ca and Mg/Ca, Sr/Ca, or U/Ca in the deepest trap (Fig. 4).

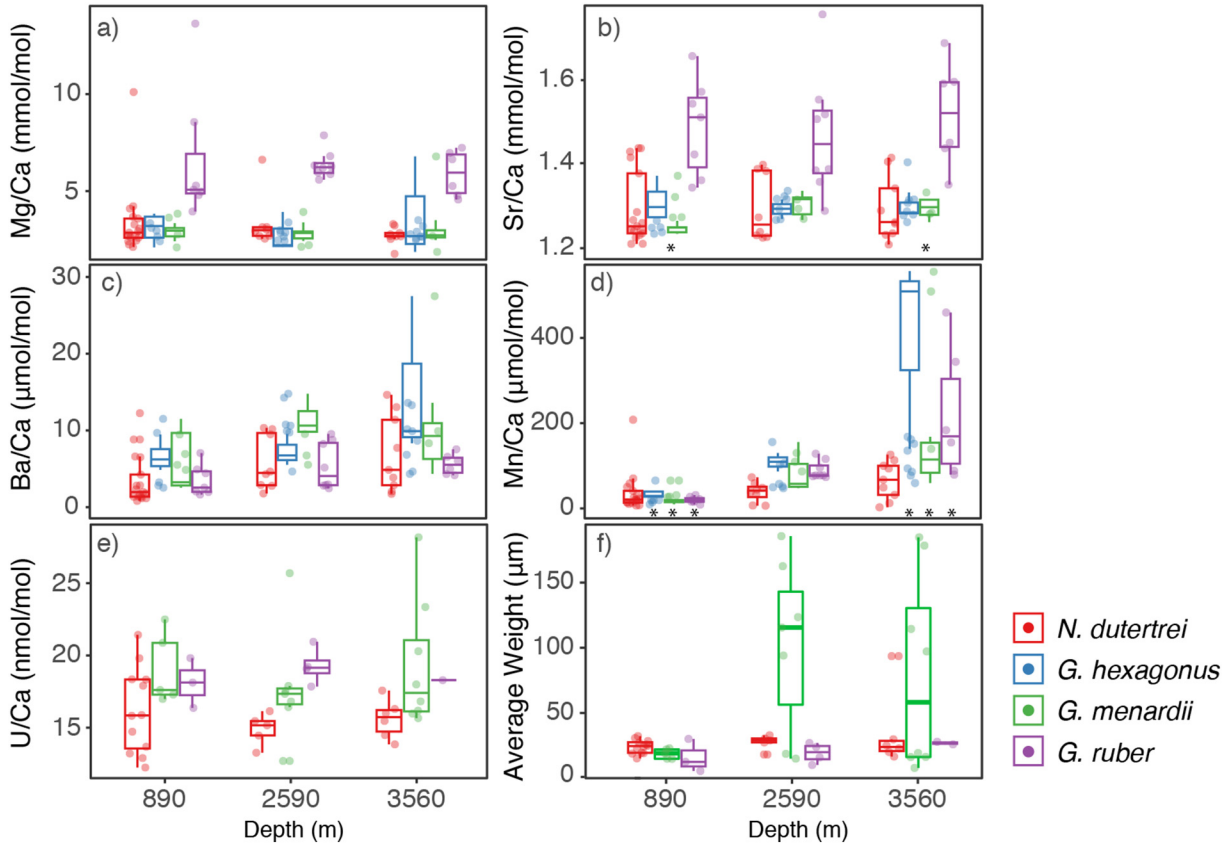

Fig. 4. Boxplots of all element to calcium ratios (a-e) and average individual foraminifera weights (f) measured in samples of sediment trap foraminifera by depth in the Panama Basin. Horizontal bars represent the sample median and boxes bound the 1st and 3rd quartiles; all data are shown as jittered points. An asterisk below the box denotes a species in which a significantly different (Kruskal-Wallis test, with Dunn's multiple comparison with Bonferroni correction; p value $< .05$) population of trace metals was identified at different depths.

Significant correlations are found between Mn/Ca and Ba/Ca in the 890 m ($r = 0.52$, p value $< .001$) and 3560 m sediment traps ($r = 0.45$, p value $= .02$) across all species, but not within a single species (Supplemental Fig. 2).

The most noticeable change with depth is an increase in the Mn/Ca values of all species, with significant differences in Mn/Ca with depth found in *G. ruber* between 890 m (mean = 18.6 ± 7.4 µmol/mol), 2590 m (mean = 88.9 ± 21.1 µmol/mol) (p value = .002), and 3560 m (mean = 216.9 ± 151.9 µmol/mol) (p value < .001), *G. menardii* between 890 m (mean = 15.3 ± 4.4 µmol/mol) and 3560 m (mean = 115.3 ± 42.4 µmol/mol) (p value = .004), and in *G. hexagonus* between 890 m (mean = 36.4 ± 18.6 µmol/mol) and 3560 m (mean = 400.4 ± 228.2 µmol/mol) (p value = .01) (Fig. 4d; Table 1). An increase in Mn/Ca with depth is also apparent in *N. dutertrei*, although differences between populations at different depths are not significant (Fig. 4d; Table 1; Supplemental Fig. 3).

Given differences in Mn/Ca values with increasing depth, we further examined if increasing Mn/Ca may be an artifact of preservation within the sediment trap itself. Cups within sediment traps open sequentially, such that material in Cup 1 (December–January) will have been in a sediment trap environment for 8–12 months longer than material captured in Cup 6 (October–November). If exposure to preservatives or the sediment trap environment are an important contributor to elevated Mn/Ca, we would expect to see an increase across consecutive cups with increasing exposure time. This is not observed (Fig. 5). While a significant correlation between Mn/Ca and duration of time in the trap (Kendall correlation; p value < .01) is found for *G. ruber* in the 3560 m trap, the direction is opposite to that expected if exposure time were important. Rather the decline in Mn/Ca ratios with time is driven by the high Mn/Ca values measured in Cup 3 (April–May) (Fig. 5).

Table 1
Mean Mn/Ca ratio and standard deviation of samples of G. ruber, N. dutertrei, G. menardii, and G. hexagonus at the depths of each of the three sediments traps.

Species	Depth (m)	Mean Mn/Ca (µmol/mol)	Mn/Ca standard deviation
G. ruber	890 m	18.6	7.5
G. ruber	2590 m	88.9	21.1
G. ruber	3560 m	216.9	151.9
N. dutertrei	890 m	35.9	46.7
N. dutertrei	2590 m	37.5	23.3
N. dutertrei	3560 m	64.9	44.8
G. menardii	890 m	15.3	4.4
G. menardii	2590 m	80.3	41.2
G. menardii	3560 m	115.3	42.4
G. hexagonus	890 m	36.4	18.6
G. hexagonus	2590 m	107.5	21.7
G. hexagonus	3560 m	400.4	228.2

4. Discussion

4.1. Trace element seasonality in the Panama Basin

The elemental composition and flux of material to sediment traps in the Panama Basin are driven largely by the seasonal migration of the Intertropical Convergence Zone (ITCZ) (Honjo, 1982; Thunell and Reynolds, 1984; Rodriguez-Rubio et al., 2002; Martinez et al., 2007; Tedesco et al., 2007; Elmore et al., 2009). When the ITCZ is at its southernmost extent (~February–April), the Panama Basin experiences upwelling and an increase in productivity (Pennington et al., 2006) that

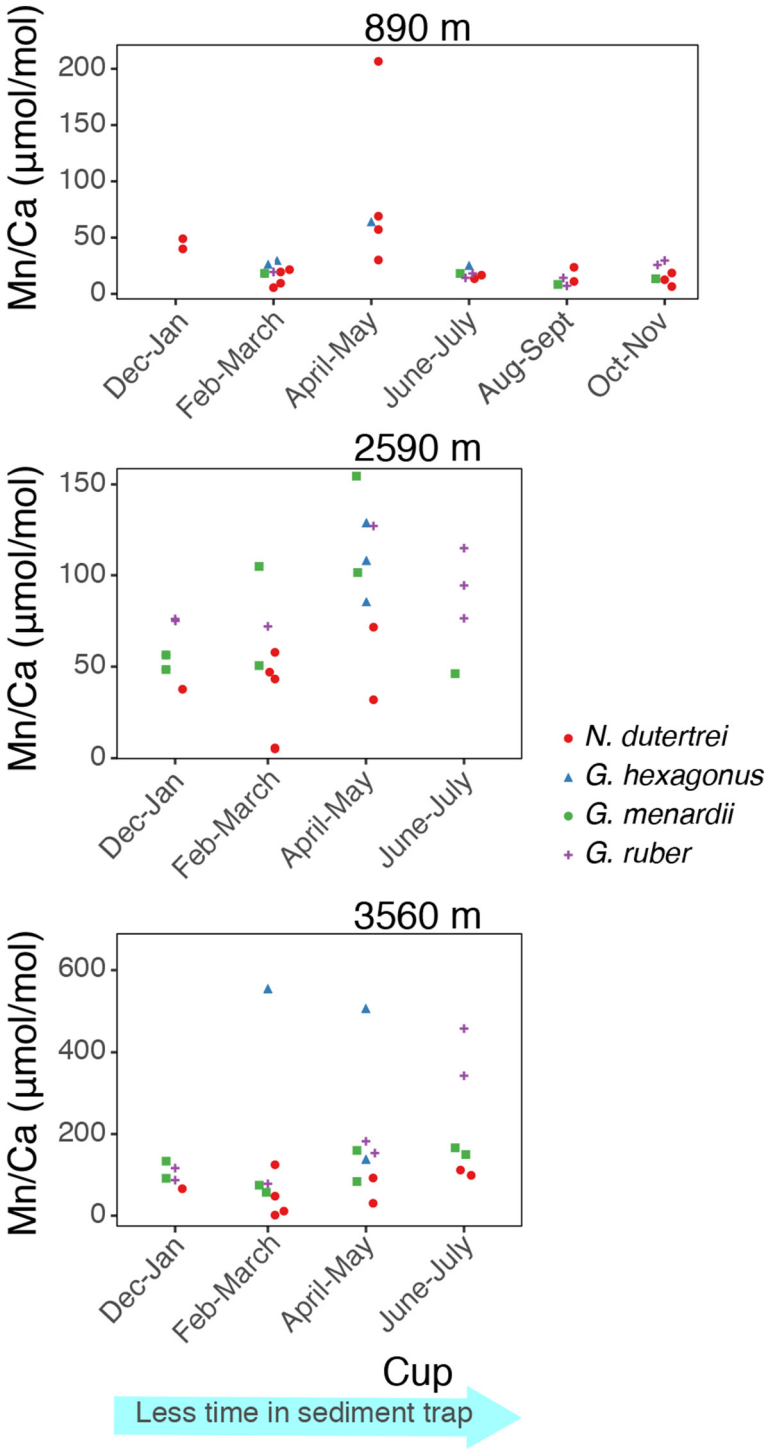

Fig. 5. Mn/Ca measured in samples of foraminifera across depths in Panama Basin shown as jittered points. Note the use of differently scaled y-axes.

is reflected in sediment traps (Curry et al., 1983; Honjo, 1982; Thunell et al., 1983; Thunell and Reynolds, 1984). All four species examined in this study, *N. dutertrei*, *G. menardii*, *G. ruber* and *G. hexagonus*, are present year round. However, non-spinose species associated with cooler waters, *N. dutertrei* and *G. menardii*, are found most abundantly in February–March, while the warmer water spinose species, *G. ruber*, is most abundant from June through September (Thunell and Reynolds, 1984).

Little seasonality is observed in most of the trace elements analyzed, in agreement with the limited variability demonstrated in the isotopic geochemistry of foraminifera from the same traps (Curry et al., 1983; Fig. 3). Ratios of Mg/Ca are largely constant within each species throughout the year, reflecting the low variability of temperatures in the upper water column. As no direct measurements of seawater properties are available in conjunction with this time series, it is not possible to compare Mg/Ca values directly to in situ temperature. However, temperature values obtained by applying paleotemperature equations to Mg/Ca ratios in *G. ruber* and *N. dutertrei*, the two species which are most frequently used as paleothermometers, are broadly consistent with modern temperatures in the upper 100 m of the Panama Basin (Fig. 1; Locarnini et al., 2018).

Sr/Ca ratios are variable in both *N. dutertrei* and *G. ruber* but with no

clear trends over time (Fig. 3b). Upwelling between February and March is a major driver of near-surface productivity in the Panama Basin, a signal that may be reflected in the lower $\delta^{13}C$ values of sub-mixed layer foraminifera during these months (Curry et al., 1983; Fig. 3f). We also find elevated Ba/Ca ratios in deeper-dwelling *N. dutertrei* and *G. menardii* from December to March (Fig. 3c), potentially reflecting upwelling and exposure to deeper, higher-Ba waters (Supplemental Fig. 4). Interestingly, U/Ca ratios in *N. dutertrei* are lower from February to May, coincident with the upwelling season, rather than in June to November (Fig. 3e). This is opposite to what might be expected in U/Ca if these species are calcifying in deeper sourced, lower pH water during upwelling intervals (Russell et al., 2004).

4.2. Heterogeneity across species

Differences in trace elemental composition across species are a reflection of both species-specific 'vital effects' and habitats. Stratification of depth habitats between shallow-dwelling *G. ruber* and the deeper-dwelling *G. menardii* and *N. dutertrei* are confirmed by the $\delta^{18}O$ and $\delta^{13}C$ values of the three species in these sediment traps (Curry et al., 1983; Patrick and Thunell, 1997; Fig. 3g) as well as their abundances in MOCNESS tows (Fairbanks et al., 1982). Oxygen isotope values are not available for *G. hexagonus* from this time series, though it is likely the deepest dwelling of the four species analyzed, found in plankton tows as deep as 1000 m in the Panama Basin (Fairbanks et al., 1982). The Mg/Ca values obtained, at least partially, reflect this depth habitat stratification with *G. ruber* values consistently higher than those of the three deeper species. Ba/Ca values are highest in the deepest-living *G. hexagonus*, followed by *N. dutertrei* and *G. menardii*, and then the shallowest species, *G. ruber* (Fig. 4c). This likely reflects depth habitat stratification and differing exposure to deeper Ba-rich waters (Sugiyama et al., 1984; Monnin et al., 1999; Fig. S4). In contrast, Sr/Ca values are similar in *G. ruber* and *G. hexagonus*, but dissimilar to *N. dutertrei* and *G. menardii* (Fig. 4b). This suggests that Sr uptake may be linked to vital effects associated with more subtle differences in ecology between species. Mn/Ca values are not significantly different among species from the 890 m trap (Fig. 4d).

4.3. Evidence for alteration of shells and trace metals in the water column

Previous work with the Panama Basin sediment trap array has shown that dissolution in the water column is minimal or absent, with neither the total flux nor average weight of foraminiferal shells attenuating with depth (Thunell et al., 1983; Thunell and Reynolds, 1984). The foraminifera analyzed here similarly show no change in shell weight with depth (Fig. 4f). However dissolution experiments do show a loss of foraminiferal calcite when samples were suspended in the water column for ~4 months below the 2590 m trap (Thunell et al., 1981), a longer exposure than that experienced by shells preserved in sediment traps.

A significant increase in both Mn/Ca values and variability is observed with increasing depth (Table 1; Fig. 4d). If the increase in Mn/Ca were due to poor preservation at depth in sediment traps, we would expect to also observe Mn/Ca ratios increasing with time spent in the trap cup. Rather, a simultaneous maximum in Mn/Ca is observed across all traps in April–May (Fig. 5). This indicates either the temporary export of shells with exceptionally high Mn/Ca ratios from the near-surface or the existence of episodic conditions within the water column that are particularly conducive to Mn/Ca scavenging. Interestingly, the April–May peak in Mn/Ca does not coincide with any event or environmental driver captured in the time series such as upwelling or productivity maxima. February–March would be the months most associated with upwelling in the Panama Basin, supported by high carbon flux and an abundance of upwelling associated *N. dutertrei* in the sediment trap (Honjo, 1982; Thunell and Reynolds, 1984), while June–July was marked by the highest organic carbon and terrestrial flux and a slight increase in the $\delta^{13}C$ of some planktic foraminifera (Honjo, 1982; Curry et al., 1983), Thus while the source of the transient Mn/Ca peak cannot be fully resolved, surface productivity appears an unlikely driver.

Our results indicate that trace element alteration of foraminiferal shells can occur in the water column, prior to deposition in the sediment. As relatively fresh shells are more susceptible to calcite-fluid exchange, recrystallization, and elemental overprinting (Chanda et al., 2019), exposure to Mn sources in the water column during export may make shells especially vulnerable to alteration of the Mn/Ca ratio. The largest change in trace element ratios occurs between 890 m and 3560 m, while Mn/Ca values at 2590 m appear to reflect values intermediate between the two. This suggests that alteration within the water column is progressive between 890 m and 3560 m. Whether alteration begins above 890 m is difficult to assess conclusively from this dataset, however two lines of evidence suggest that alteration may occur above 890 m. The first is the presence of an anomalously high Mn/Ca value (> 200 μmol/mol) found in one sample of *N. dutertrei*. The second is several unusually high Mg/Ca values (> 7 mmol/mol) found in both *N. dutertrei* and *G. ruber* in the 890 m trap. When converted to temperature using the *G. ruber* Mg/Ca:temperature equation of Anand et al. (2003), these Mg/Ca values result in unrealistic near-surface temperatures reaching 47 °C. Although we do not find a systematic increase in Mg/Ca with depth or covariation with Mn/Ca in our samples, the measured values are too high to represent the sea surface and may indicate additional shell alteration.

4.4. Mn/Ca adsorption in the water column

One of the most widely reported forms of trace element alteration in the foraminiferal record is the presence of Mn rich carbonate overgrowths associated with high Mg/Ca ratios (Boyle, 1983; Pena et al., 2008, Pena et al., 2005; Gibson et al., 2016). However, the increasing Mn/Ca in shells with depth in our study is not accompanied by similar changes in the Mg/Ca ratios (Fig. 6), and suggests that processes leading to the alteration of Mn/Ca in the Panama Basin water column may not impact the Mg/Ca of shells in the same manner as overgrowths that occur in the sediments. Moreover, while shells recovered from the 3650 m trap appear to show signs of some degradation (Fig. 7), there were no visible overgrowths akin to those described in sediments (Pena et al., 2005; Pena et al., 2008) or other sediment traps (Gibson et al., 2016).

Rather, our observations are consistent with Mn scavenging by sinking foraminiferal shells. Previous work has shown that Mn adsorption onto large particles, particularly biogenic carbonates, plays an important role in regional manganese cycling in the Equatorial Pacific water column (Martin and Knauer, 1983; Martin and Knauer, 1984; Murray and Leinen, 1993). Martin and Knauer (1984) demonstrate increasing particulate Mn values with increasing oxygenation below the oxygen minimum associated with scavenging of dissolved Mn onto particles (see Fig. 1 in Martin and Knauer, 1984). This is consistent with our observation of an increase in Mn/Ca occurring below the oxygen minimum zone (Fig. 2). In addition to the presence of a strong oxygen minimum zone (Klinkhammer and Bender, 1980; Martin and Knauer, 1984; Nameroff et al., 2002), exposure to high manganese in organic aggregates (Cowen and Silver, 1984; Hebel et al., 1986; Neretin et al., 2003), volcanism, and hydrothermal activity such as that associated with the Galapagos Rift (Klinkhammer et al., 1977; Lea et al., 2005) could all be additional sources of excess Mn at depth available to sinking foraminiferal shells. These later sources could increase the availability of Mn at depths below the oxygen minimum zone, accounting for the continued increase in foraminiferal Mn/Ca below the lower oxycline between 2590 and 3560 m.

The amount of Mn/Ca adsorbed onto shells is not consistent even over the short time series available, with especially high Mn/Ca values observed in April–May at all depths. Murray and Leinen (1993)

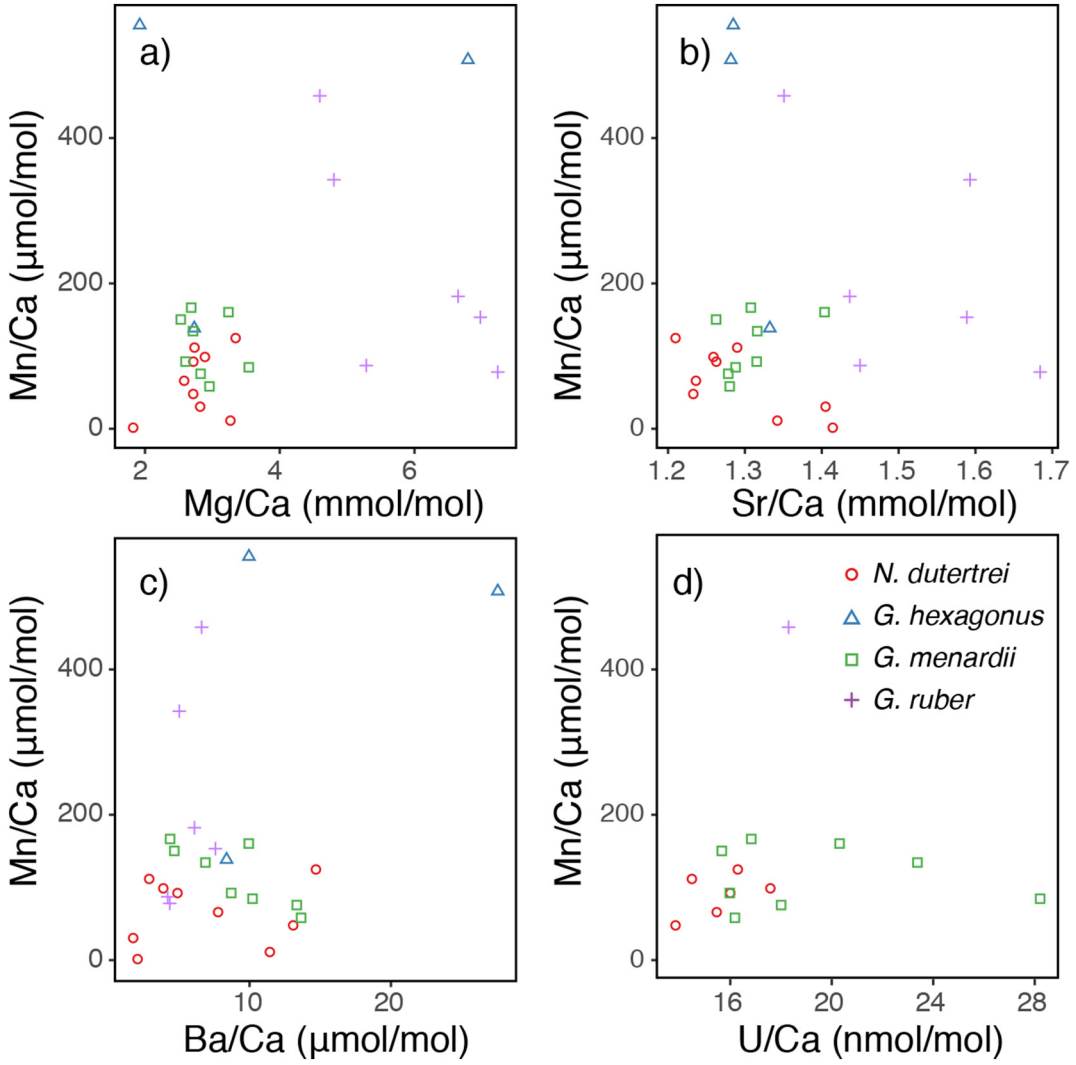

Fig. 6. Crossplots of Mn/Ca and (a) Mg/Ca, (b) Sr/Ca, (c) Ba/Ca, and (d) U/Ca from the 3560 m sediment trap. Only the correlation between Mn/Ca and Ba/Ca is significant (r = 0.45; p value = .02), but this trend is not maintained within species.

previously observed an imbalance in the $Mn/CaCO_3$ of sediments from the Equatorial Pacific, which they interpreted as a limitation in the water column Mn available for scavenging. If so, temporal differences in the amount of Mn/Ca adsorbed onto fresh foraminiferal shells may be a reflection of Mn cycling in the water column. Unfortunately, contemporaneous Mn measurements from the water column do not exist, and linking geochemical alterations of shells directly to conditions in the water column will require analyses of material from other deep sediment trap deployments.

Our results further show that thinner walled, lightly calcified species are more susceptible to alteration in the water column. In the Panama Basin, Mn/Ca ratios are not significantly different between populations of *N. dutertrei* recovered from different depths, and the increase in Mn/Ca with depth in *G. menardii* is smaller than in either of the more lightly calcified species *G. ruber* or *G. hexagonus* (Fig. 4d; Supplemental Fig. 3). There are two possible reasons for lightly calcified species to be more affected by geochemical alteration. Thinner shells have a similar surface area exposed to overgrowths, dissolution, and adsorption, but lower overall calcite volume. Thus surface alteration of the geochemistry of a thin walled species will have a greater impact on whole shell geochemistry. Compounding this effect are differences in sinking rate, with heavier, denser species, spending less time in the water column (Takahashi, 1984).

High Mn/Ca ratios have previously been reported in foraminifera from Panama Basin sediments linked to carbonate overgrowths on shells (e.g., Boyle, 1983; Pena et al., 2005; Pena et al., 2008; Tachikawa et al., 2013; Umling et al., 2018). While these results suggest that alteration during transport is a potentially important source of high Mn/Ca measured in Panama Basin foraminifera, we reiterate that this is distinct from the diagenetic processes resulting in high Mn/Ca described previously. Mn/Ca ratios from uncleaned planktic foraminifera from nearby sediment cores frequently show visible carbonate overgrowths, covariation between Mg/Ca and Mn/Ca ratios, and markedly higher Mn/Ca than the sediment trap specimens measured here, with benthic foraminifera also showing elevated Mn/Ca (Umling and Thunell, 2017). For example, a mean Mn/Ca of 520 µmol/mol is reported in the Panama Basin core TR163-20B by Umling et al. (2018), while uncleaned foraminifera from ODP 1240 are reported to have Mn/Ca > 580 µmol/mol (Pena et al., 2008). This is a factor of 4 to 5 times higher than our mean Mn/Ca value of 154 µmol/mol in the 3560 m trap.

5. Conclusions and implications for proxy interpretation

The results of trace elemental analyses of four species of foraminifera from sediment traps at multiple depths in the Panama Basin provide evidence that post-mortem alteration of foraminiferal calcite is not confined to the sediment, but can occur rapidly during export

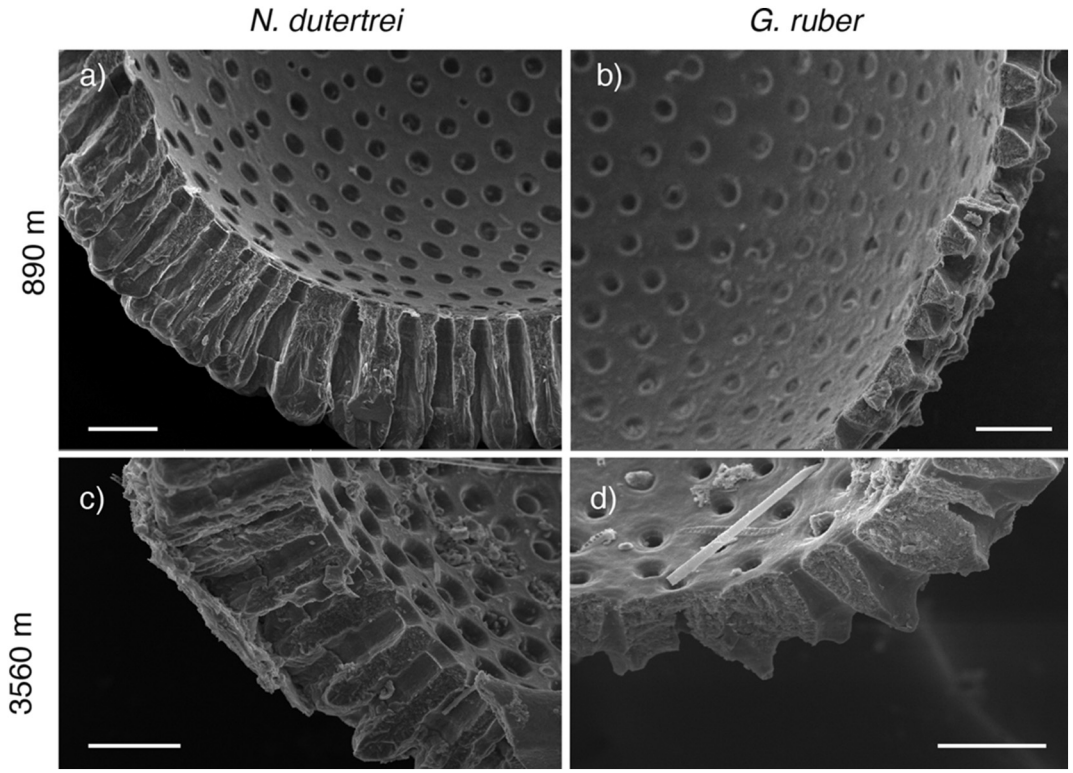

Fig. 7. SEM images on the shell wall and inner surface of *N. dutertrei* (a,c) and *G. ruber* (b,d) from the Panama Basin. Images (a) and (b) are of foraminifera recovered from the 890 m trap and appear relatively pristine. Images (c) and (d) are typical of shells recovered from the 3560 m trap, showing some pitting but no overgrowths. Scale bars of 20 μm are shown in white for each image.

through the water column. If increases in Mn with depth are due to adsorption of Mn onto carbonate shells, much of this signal should be removed by the weak acid leach step included in most 'cleaning' protocols prior to solution ICP-MS analyses of fossil foraminifera (Barker et al., 2003). As it is already common practice to subject sedimentary samples of planktic foraminifera to rigorous cleaning, our findings should not necessarily alter the way in which this type of geochemical proxy data for near-surface conditions is obtained or interpreted.

Although the mechanisms responsible for alteration of calcite in the water column and in sediments are likely distinct, it is unclear if or how trace element alteration occurring within the water column could be differentiated from that occurring in the sediment in fossil shells. This may be further complicated if Mn, initially scavenged during transport, is a driver of Mn availability in the sedimentary microenvironment where shells undergo further diagenesis. Thus Mn adsorbtion in the water column may act as an indirect contributor to high Mn in carbonate overgrowths. In fact, as recrystallization occurs more readily in fresh shells (Chanda et al., 2019), early exposure to elevated Mn in the immediate microenvironment may make shells more susceptible to incorporation of high Mn in recrystallized calcite. Importantly, our findings show that geochemical alterations of foraminiferal shells, including elevated Mn/Ca, are not necessarily indicative of bottom water conditions alone, and may be influenced by conditions within the overlying water column, including the availability of Mn in the ambient environment, and/or within sinking aggregates in which foraminifera may be entrained.

Author statement

C. Davis conceived of this study and did the formal analysis. Both C. Davis and C. Benitez-Nelson participated in data analysis and the writing and editing of the manuscript.

Declaration of Competing Interest

Authors have no conflicts of interest.

Acknowledgements

We'd like to thank A. Stevenson and B. Morse for their assistance in sample preparation. This manuscript was improved by the comments of an anonymous reviewer. Support for this work was provided by NSF OCE #1631977.

Appendix A. Supplementary data

Supplementary data to this article can be found online at https://doi.org/10.1016/j.marmicro.2020.101872.

References

Allen, K.A., Honisch, B., Eggins, S.M., Haynes, L.L., Rosenthal, Y., Yu, J., 2016. Trace element proxies for surface ocean conditions: a synthesis of culture calibrations with planktic foraminifera. Geochim. Cosmochim. Acta 193 (15), 197–221.

Anand, P., Elderfield, H., Conte, M.H., 2003. Calibration of Mg/Ca thermometry in planktonic foraminifera from a sediment trap time series. Paleoceanography 18 (2), 1050–1065.

Barker, S., Greaves, M., Elderfield, H., 2003. A study of cleaning procedures used for foraminiferal Mg/Ca paleothermometry. Geochem. Geophys. Geosyst. 4 (9), 8407–8427.

Benway, H.M., Haley, B., Klinkhammer, G.P., Mix, A.C., 2003. Adaptation of a flow-through leaching procedure for Mg/Ca paleothermometry. Geochem. Geophys. Geosyst. 4 (2).

Boiteau, R., Greaves, M., Elderfield, H., 2012. Authigenic uranium in foraminiferal coatings: a proxy for ocean redox chemistry. Paleoceanography 27, PA3227. https://doi.org/10.1029/2012PA002335.

Boyle, E.A., 1983. Manganese carbonate overgrowths on foraminifera tests. Geochim. Cosmochim. Acta 47 (10), 1815–1819.

Boyle, E.A., Keigwin, L.D., 1985. Comparison of Atlantic and Pacific paleochemical records for the last 215,000 years: Change in deep ocean circulation and chemical inventories. Earth Planet. Sci. Lett. 76, 135–150.

Branson, Oscar, et al., 2019. LAtools: A data analysis package for the reproducible reduction of LA-ICPMS data. Chemical Geology 504, 83–95. https://doi.org/10.1016/j.chemgeo.2018.10.029.
Chanda, P., Gorski, C.A., Oakes, R.L., Fantle, M.S., 2019. Low temperature stable mineral recrystallization of foraminiferal tests and implications for the fidelity of geochemical proxies. Earth Planet. Sci. Lett. 506, 428–440.
Cleroux, C., Cortijo, E., Anand, P., Labeyrie, L., Bassinot, F., Caillon, N., Duplessy, J.-C., 2008. Mg and Sr/ca ratios in planktonic foraminfiera: proxies for upper water column temperature reconstruction. Paleoceanogr. Paleoclimatol. 23 (3). https://doi.org/10.1029/2007PA001505.
Cowen, J.P., Silver, M.W., 1984. The association of iron and manganese with bacteria on marine macroparticulate material. Science 224 (4655), 1340–1342.
Curry, W.B., Thunell, R.C., Honjo, S., 1983. Seasonal changes in the isotopic composition of planktonic foraminifera collected in Panama Basin sediment traps. Earth Planet. Sci. Lett. 64 (1), 33–43.
Dekens, P.S., Lea, D.W., Pak, D.K., Spero, H.J., 2002. Core top calibration of Mg/Ca in tropical foraminifera: refining paleotemperature estimation. Geochem. Geophys. Geosyst. 3 (4), 1–29.
Dunn, O.J., 1961. Multiple comparisons using rank sums. Technometrics 6, 241–252.
Elderfield, H., Ganssen, G., 2000. Past temperature and $\delta^{18}O$ of surface ocean waters inferred from foraminiferal Mg/Ca ratios. Nature 405 (6785), 442–445.
Elmore, A.C., Thunell, R.C., Styles, R., Black, D., Murray, R.W., Martinez, N., Astor, Y., 2009. Quantifying the seasonal variations in fluvial and eolian sources of terrigenous material to Cariaco Basin, Venezuela. J. S. Am. Earth Sci. 27 (2–3), 197–210.
Fairbanks, R.G., Sverdlove, M., Free, R., Wiebe, P.H., Be, A.W.H., 1982. Vertical distribution and isotopic fractionation of living planktonic foraminifera from the Panama Basin. Nature 298, 841–844.
Fraile, I., Mulitza, S., Schulz, M., 2009. Modeling planktonic foraminiferal seasonality: implications for sea-surface temperature reconstructions. Mar. Micropaleontol. 72 (2), 1–9.
Gibson, K.A., Thunell, R.C., Machain-Castilla, M.L., Fehrenbacher, J., Spero, H.J., Wejnert, K., Nava-Fernandez, X., Tappa, E.J., 2016. Evaluating controls on planktonic foraminiferal geochemistry in the Eastern Tropical North Pacific. Earth Planet. Sci. Lett. 452, 90–103.
Gottschalk, J., Skinner, L.C., Lippold, J., Vogel, H., Frank, N., Jaccard, S.L., Waelbroeck, C., 2016. Biological and physical controls in the Southern Ocean on past millennial-scale atmospheric CO_2. Nat. Commun. 7, 11539. https://doi.org/10.1038/ncomms11539.
Hebel, D., Knauer, G.A., Martin, J.H., 1986. Trace metals in large agglomerates (marine snow). J. Plankton Res. 8 (4), 819–824.
Honjo, S., 1982. Seasonality and Interaction of biogenic and lithogenic particulate flux at the Panama Basin. Science 218 (4575), 883–884.
Jonkers, L., Kucera, M., 2015. Global analysis of seasonality in the shell flux of extant planktonic foraminifera. Biogeosciences 12 (7), 2207–2226.
Katz, M.E., Cramer, B.S., Franzese, A., Hönisch, B., Miller, K.G., Rosenthal, Y., Wright, J.D., 2010. Traditional and emerging geochemical proxies in foraminifera. J. Foraminiferal Res. 40 (2), 165–192.
Klinkhammer, G.P., Bender, M.L., 1980. The distribution of manganese in the Pacific Ocean. Earth Planet. Sci. Lett. 46, 361–384.
Klinkhammer, G.P., Bender, M., L., & Weiss, R.F., 1977. Hydrothermal manganese in the Galapagos Rift. Nature 269, 319–320.
Lea, D.W., 1999. Trace elements in foraminiferal calcite. In: Modern Foraminifera. Springer, Dordrecht.
Lea, D.W., Pak, D.K., Paradis, G., 2005. Influence of volcanic shards on foraminiferal Mg/Ca in a core from the Galapagos region. Geochem. Geophys. Geosyst. 6https://doi.org/10.1029/2005GC000970. Q11P04.
Locarnini, R.A., Mishonov, A.V., Baranova, O.K., Boyer, T.P., Zweng, M.M., Garcia, H.E., Reagan, J.R., Seidov, D., Weathers, K., Paver, C.R., Smolyar, I., 2018. WorldOcean Atlas 2018, Volume 1: Temperature, A. Mishonov Technical ed. 81. NOAA Atlas NESDIS, pp. 52.
Marr, J.P., Bostock, H.C., Carter, L., Bolton, A., Smith, A., 2013. Differential effects of cleaning procedures on the trace element chemistry of planktonic foraminifera. Chem. Geol. 351, 310–323.
Martin, J.H., Knauer, G.A., 1983. VERTEX: manganese transport with $CaCO_3$. Deep-Sea Res. 30 (4), 411–425.
Martin, J.H., Knauer, G.A., 1984. VERTEX: manganese transport through oxygen minimua. Earth Planet. Sci. Lett. 67, 35–47.
Martinez, N.C., Murray, R.W., Thunell, R.C., Peteson, L.C., Muller-Karger, F., Astor, Y., Varela, R., 2007. Modern climate forcing of terrigenous deposition in the tropics (Cariaco Basin, Venezuela). Earth Planet. Sci. Lett. 264 (3–4), 438–451.
Mashiotta, T.A., Lea, D.W., Spero, H.J., 1999. Glacial–interglacial changes in Subantarctic Sea surface temperature and δ18O-water using foraminiferal Mg. Earth Planet. Sci. Lett. 170 (4), 417–432.
McConnell, M.C., Thunell, R.C., 2005. Calibration of the planktonic foraminiferal Mg/Ca paleothermometer: sediment trap results from the Guaymas Basin, Gulf of California. Paleoceanography 20 (2).
Monnin, C., Jeandel, C., Cattaldo, T., Dehairs, F., 1999. The marine barite saturation state of the world's oceans. Mar. Chem. 65, 253–261.
Murray, R.W., Leinen, M., 1993. Chemical transport to the seafloor of the equatorial Pacific Ocean across a latitudinal transect at 135°W: tracking sedimentary major, trace, and rare earth element fluxes at the equator and the intertropical convergence zone. Geochim. Cosmochim. Acta 57, 4141–4163.
Nameroff, T.J., Balistrieri, L.S., Murray, J.W., 2002. Suboxic trace metal geochemistry in the Eastern Tropical North Pacific. Geochim. Cosmochim. Acta 66 (7), 1139–1158.
Neretin, L.N., Pohl, C., Jost, G., Leipe, T., Pollehne, F., 2003. Manganese cycling in the Gotland deep, Baltic Sea. Mar. Chem. 82, 125–143.
Nurnberg, D., Bijma, J., Hemleben, C., 1996. Assessing the reliability of magnesium in foraminiferal calcite as a proxy for water mass temperatures. Geochimica et Cosmochimica 60 (5), 803–814.
Palmern, M.R., Elderfield, H., 1986. Rare earth elements and neodymium isotopes in ferromanganese oxide coatings of Cenozoic foraminifera from the Atlantic Ocean. Geochim. Cosmochim. Acta 50 (3), 409–417.
Patrick, A., Thunell, R.C., 1997. Tropical Pacific sea surface temperatures and upper water column thermal structure during the last glacial maximum. Paleoceanography 12 (5), 649–657.
Pena, L.D., Calvo, E., Cacho, I., Eggins, S., Pelejero, C., 2005. Identification and removal of Mn-Mg-rich contaminant phases on foraminiferal tests: implications for Mg/Ca past temperature reconstructions. Geochem. Geophys. Geosyst. 6 (9).
Pena, L.D., Cacho, I., Calvo, E., Pelejero, C., Eggins, S., Sadekov, A., 2008. Characterization of contaminant phases in foraminifera carbonates by electron microprobe mapping. Geochem. Geophys. Geosyst. 9 (7).
Pennington, J.T., Mahoney, K.L., Kuwahara, V.S., Kolber, D.D., Calienes, R., Chavez, F.P., 2006. Primary productivity in the eastern tropical Pacific: a review. Prog. Oceanogr. 69, 285–317.
Regenberg, M., Steph, S., Nürnberg, D., Tiedemann, R., Garbe-Schönberg, D., 2009. Calibrating Mg/Ca ratios of multiple planktonic foraminiferal species with $\delta^{18}O$-calcification temperatures: Paleothermometry for the upper water column. Earth Planet. Sci. Lett. 278 (3–4), 324–336.
Reichart, G.-J., Jorissen, F., Anschutz, P., Mason, P.R.D., 2003. Single foraminiferal test chemistry records the marine environment. Geology 31 (4), 355–358.
Rodriguez-Rubio, E., Schneider, W., Abarca del Rio, R., 2002. On the seasonal circulation within the Panama Bight derived from satellite observations of wind, altimetry, and sea surface temperature. Geophys. Res. Lett. 30 (7), 1410–1414.
Russell, A.D., Honisch, B., Spero, H.J., Lea, D.W., 2004. Effects of seawater carbonate ion concentration and temperature on shell U, Mg, and Sr in cultured planktonic foraminifera. Geochim. Cosmochim. Acta 68 (21), 4347–4361.
Sexton, P.F., Wilson, P.A., Pearson, P.N., 2006. Microstructural and geochemical perspectives on planktic foraminiferal preservation: "Glassy" versus "Frosty". Geochem. Geophys. Geosyst. 7 (12) Q12P19.
Sugiyama, M., Matsui, M., Nakayama, E., 1984. Direct determination of Barium in sea water by inductively coupled plasma emission spectrometry. J. Oceanogr. Soc. Jpn 40, 295–302.
Tachikawa, K., Toyofuku, T., Basile-Doelsch, I., Delhaye, T., 2013. Microscale neodymium distribution in sedimentary planktonic foraminiferal tests and associated mineral phases. 100. pp. 11–23.
Takahashi, K., Be, A.W.H., 1984. Planktonic foraminifera: factors controlling sinking speeds. Deep Sea Res. A. Oceanogr. Res. Papers 31 (12), 1477–1500.
Tedesco, K., Thunell, R.C., Astor, Y., Muller-Karger, F., 2007. The oxygen isotope composition of planktonic foraminifera from the Cariaco Basin, Venezuela: Seasonal and interannual variations. Mar. Micropaleontol. 62 (3), 180–193.
Thunell, R.C., Reynolds, L.A., 1984. Sedimentation of planktonic foraminifera: seasonal changes in species flux in the Panama Basin. Micropaleontology 243–262.
Thunell, R.C., Keir, R.S., Honjo, S., 1981. Calcite dissolution: an in situ study in the Panama Basin. Science 212 (4495), 659–661.
Thunell, R.C., Curry, W.B., Honjo, S., 1983. Seasonal variation in the flux of planktonic foraminifera: time series sediment trap results from the Panama Basin. Earth Planet. Sci. Lett. 64 (1), 44–55.
Umling, N.E., Thunell, R.C., 2017. Synchronous deglacial thermocline and deep-water ventilation in the eastern equatorial Pacific. Nat. Commun. 8, 14203. https://doi.org/10.1038/ncomms14203.
Umling, N.E., Thunell, R.C., 2018. Mid-depth respired carbon storage and oxygenation of the eastern equatorial Pacific over the last 25,000 years. Quat. Sci. Rev. 189, 43–56.
Umling, N.E., Thunell, R.C., Bizimis, M., 2018. Deepwater expansion and enhanced remineralization in the Eastern Equatorial Pacific during the last Glacial Maximum. Paleoceanogr. Paleoclimatol. 33, 563–578.
von Langen, P.J., Pak, D., Spero, H.J., Lea, D.W., 2005. Effects of temperature on Mg/Ca in Neogloboquadrinid shells determined by live culture. Geochem. Geophys. Geosyst. 61 (10). https://doi.org/10.1029/2005GC000989.